Shock Waves (2003) 13: 33–40
Digital Object Identifier (DOI) 10.1007/s00193-003-0180-7

Shock Waves

Attenuation of shock waves by granular filters

J. Bakken[1], T. Slungaard[2], T. Engebretsen[3], S.O. Christensen[4]

[1] Complex Flow Design AS, P.O. Box 1273, 7462 Trondheim, Norway
[2] NTNU, Department of Energy and Process Engineering, Kolbjørn Hejes vei 1A, 7491 Trondheim, Norway
[3] SINTEF Materials Technology, R. Birkelands vei 2b, 7465 Trondheim, Norway
[4] Norwegian Defence Estates Agency, Oslo Mil/Akershus, 0015 Oslo 1, Norway

Received 30 September 2002 / Accepted 19 December 2002
Published online 6 March 2003 –

Abstract. Attenuation of shock waves in granular filters has been studied. Both pressurized air and solid explosives have been used for generating shock waves in a shock tube. The shock tube had a total length of ∼22 m, and an internal diameter of 355 mm. Two large scale experiments have also been carried out in a tunnel with a cross-sectional area of 6.5 m^2. The results are compared with results found in the literature (Zloch, 1976; Medvedev et al., 1990; Britan et al., 2001) and previous experiments in a smaller scale by Slungaard (2002). A simple correlation based on the work of Zloch (1976) for shock wave attenuation in tube bundles and an extensive amount of experiments, is proposed. The correlation $p_2/p_1 = 1/(1+\theta/B)$ can be used to estimate the attenuation of the shock wave through a granular filter with filter characteristic θ. Setting B=6 will give a conservative estimate of the attenuation, while setting B=3 will give the best fit to all the results from this study and the results found in the literature. The correlation is independent of the type of driver (pressurised air or solid explosives) and upstream shock strength.

Key words: Shock waves, Granular filter, Attenuation, Pressure drop

1 Introduction

When gas flows through a bed of granular media, it is subjected to a pressure drop. The classical correlation used for solving this problem is given by Ergun (1952). The Ergun equation is later modified by several others (for example Macdonald et al., 1979; Idelchik, 1994). The purpose of this work is not to present another modification of the Ergun equation, but to use it as a basis for calculation of shock wave attenuation through a granular bed, or filter. The goal is to establish a simple correlation that can be used to estimate the attenuation of a shock wave through a granular filter.

First some dimensionless numbers needed in the further treatment must be defined. The modified Reynolds number is expressed as:

$$Re_m = \frac{Re}{1-\epsilon} = \frac{\rho u d}{\mu(1-\epsilon)} \tag{1}$$

where ϵ is the void fraction, ρ is the gas density [kg/m^3], u is the superficial gas velocity [m/s], d is the particle diameter [m] and μ is the dynamic viscosity [Ns/m^2].

A modified pressure drop coefficient can be defined as:

$$f_m = \frac{\Delta p}{\rho u^2} \cdot \frac{d}{L} \cdot \frac{\epsilon^3}{(1-\epsilon)} \tag{2}$$

where Δp is the pressure drop through the filter [Pa] and L is the filter length [m].

The modified pressure drop coefficient can be correlated as:

$$f_m = \alpha \left(\frac{Re}{1-\epsilon} \right)^{-1} + \beta = \frac{\alpha}{Re_m} + \beta \tag{3}$$

which is the classical Ergun equation. Ergun (1952) estimated α to be 150 and β to be 1.75. MacDonald et al. (1979) later found α to be 180 and $1.8 < \beta < 4.0$, with the smallest β for smooth particles and the largest β for the roughest particles. In the current work and the work by Slungaard (2002), β is also found to depend on the filter material, as shown in Fig. 1. As can be seen from this figure, or Eq. (3), f_m approaches a constant value that is equal to β for high Reynolds numbers. When the modified Reynolds number is known, Fig. 1 (or Eq. (3)) and Eq. (2) can be used to calculate the head loss for steady gas flow through the filter.

The objective of the present work is to predict the shock wave attenuation through a granular filter with a simple correlation that is independent of the incoming shock strength and driver type. Since granular filters can

Correspondence to: J. Bakken
(e-mail: Jorn.Bakken@complex-flow.com)

be of different sizes (length and diameter) with different particles (size, shape, roughness, density etc.), it would be convenient to characterize the filter by a single number. According to Medvedev et al. (1990) the shock wave strength downstream of the granular filter depends on the upstream Mach number and the dimensionless filter characteristic. The filter characteristic is defined as:

$$\theta = f_m \cdot \frac{(1-\epsilon)}{\epsilon} \cdot \frac{L}{d} \,. \tag{4}$$

When dealing with shock waves, the Reynolds number will always be so high that f_m is constant (i.e. only depending on β). Medvedev et al. (1990) use the approach of a high Reynolds number, and set f_m=1.75. This is equal to a β value as suggested by Ergun (1952) (Eq. (3)).

Britan et al. (2001) use only the non-dimensional filter length (L/d) when presenting their data. They also present a numerical solution which represents the experimental findings well. The curve representing the numerical solution is close to $p_2/p_1 = 0.6(L/d)^{-0.54}$. Britan et al. (2001) found that for short filters ($\theta \leq 15$) the results were in good agreement with the data from Medvedev et al. (1990). However, for longer filters the experimental results were closer to those of Engebretsen et al. (1996). Table 1 shows the experimental conditions for Britan et al. (2001) and Medvedev et al. (1990) (and also Slungaard (2002) and Zloch (1976)).

Slungaard (2002) repeated the experiments with 15 mm glass spheres by Engebretsen et al. (1996).[1] The results differed significantly from what was achieved by Engebretsen et al. (1996). A closer examination of the original data from Engebretsen has convinced us that these data should be rejected. The reason for this can be attributed to the data acquisition system. This is further discussed in the Appendix.

Besides the work of Medvedev et al. (1990), Britan et al. (2001) and Slungaard (2002), very little experimental work has been carried out in this area. However, Zloch (1976) also performed some experiments. Although the major part of the experiments were performed with tube bundles representing the granular filter, some experiments with spherical pebbles were also performed. Some tests with tube bundles were also performed by Bakken (1995). Bakken (1995) used a detonation driver in his experiments, and the OAR (Open Area Ratio) was much larger than in the experiments by Zloch (1976).

In this work the approach of a high Reynolds number has been adopted, and f_m is assumed to be constant for all experiments in this study and the experiments found in the literature (Zloch, 1976; Medvedev et al., 1990; Britan et al., 2001; Slungaard, 2002). In this study we have chosen to use only two constant values for f_m as shown in Fig. 1 ($f_m = 1$ for spherical particles and $f_m = 2.5$ for crushed rock). Using $f_m = 1$ for spherical particles differs from Medvedev et al. (1990). It should, however, be pointed out that particles can have different degrees of spherical shape, so using only two distinct values for f_m is somewhat artificial. In reality f_m decreases continuously from $f_m = 2.5$ for crushed rock towards $f_m = 1.0$ as the shape becomes more spherical.

[1] These experiments were also presented by Slungaard et al. (1998), and a closer discussion is given by Slungaard (2002).

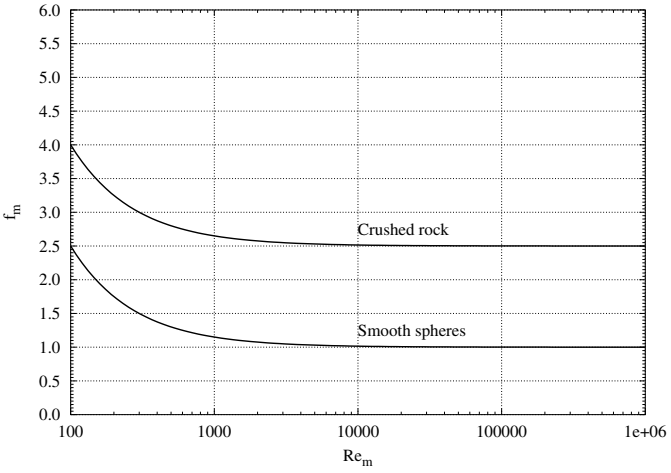

Fig. 1. Pressure drop coefficient as a function of the modified Reynolds number (Slungaard, 2002). $\alpha = 150$ and $\beta = 1$ or 2.5

Based on experiments it is shown that the attenuation of shock waves through a granular filter can be expressed as a function of this filter characteristic.

2 Experimental setup

The major part of the experiments has been carried out in a shock tube. The shock tube has a total length of ∼22 m and is closed at both ends. The internal diameter is 355 mm. To generate the shock wave either pressurized air or a solid explosive has been used. It is also possible to use a gaseous detonation driver, but this has not been a part of this study.

Two large scale experiments have also been carried out in a tunnel with a cross-sectional area of 6.5 m^2. In this case a solid explosive was used to generate the shock wave.

2.1 Shock tube

Figure 2 shows a sketch of the shock tube. Two lengths are shown, the first one corresponds to tests with pressurized air, while the second corresponds to tests with solid explosives. The position of the pressure transducers are also shown relative to the inlet of the granular filter. The filter length was varied from 150 mm to 870 mm. The filter material was rocks with an arbitrary shape and volume averaged diametres of 18.8 mm and 53.9 mm, respectively. The filters tested are shown in Table 2. The volume average diameter and the density, was found by submerging a representative selection of the rocks in water, and then weighing the rocks. Since the total volume of the filter was known, the void fraction of each filter could be found by weighing the whole filter.

The shock tube was equipped with four Kulite XT190 and four Kistler 603B pressure transducers positioned as shown in Fig. 2. The pressure transducers are numbered

Table 1. Experimental conditions from Zloch, 1976; Medvedev et al., 1990; Britan et al., 2001; Slungaard, 2002

Ref	Zloch, 1976	Medvedev et al., 1990	Britan et al., 2001	Slungaard, 2002
Particle shape	Spherical	Spherical	Spherical	Spherical
Particle diameter (mm)	Not given	3.9–21.9	0.5–4.4	15 and 41
Filter lenght (mm)	Not given	10–250	4–63	125–380
Shock strength (MPa)	0.25,0.41 (M = 1.5,1.9)	0.13–0.25 (M = 1.1–1.5)	0.23 (M = 1.46)	0.7–2.7
θ	0.4–34	1.7–25	2–92	3–37

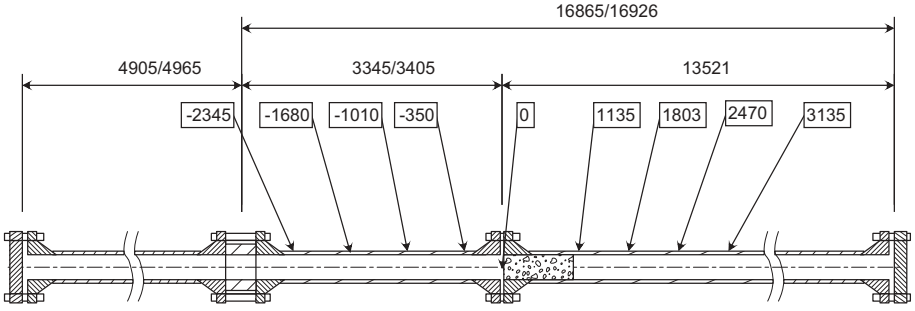

Fig. 2. Sketch of the shock tube and location of pressure transducers. Dimensions and positions in millimetres

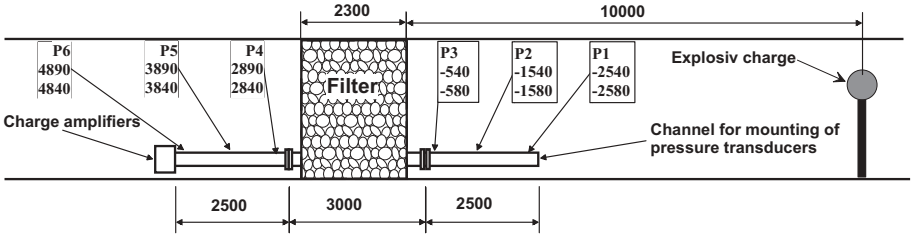

Fig. 3. Sketch of the large scale setup. Dimensions and positions in millimetres

Table 2. Description of filters

Filter length (mm)	Particle diameter (mm)	Void fraction	θ
150	18.8	0.44	25.4
300	18.8	0.39	62.4
300	53.9	0.45	17.0
450	18.8	0.41	86.1
600	53.9	0.46	32.7
870	53.9	0.46	47.4

P1 to P8 from left to right. All pressure transducers were connected to amplifiers and further to a digital oscilloscope for recording and storing of data. The oscilloscope was triggered by arrival of the shock wave at the first pressure transducer.

When pressurized air is used, the length of the driver section is ∼5 m. A steel diaphragm is used to separate the driver from the acceptor section (see Fig. 2). The pressure in the driver is gradually increased until the diaphragm bursts. Two different driver pressures were used in the present tests, 1 and 5 MPa. [2]

[2] All pressures refers to pressure above atmospheric pressure.

When a solid explosive is used to generate the shock wave, the charge is placed in the centre of the tube ∼5 m from the left end wall (see Fig. 2). In the current tests, two different charges were used, 10 g and 30 g of C-4. These charges were selected to give the same incoming pressure to the filter as the pressurized air driver. However, the incoming pressures were somewhat lower than expected. For both driver types, the distance from the diaphragm, or the explosive charge, to the inlet of the granular filter is just below 10 diameters.

2.2 Large scale

Two large scale experiments have also been conducted. In this case the granular filter was built in an underground tunnel 730 m below the surface. The frontal area of the filter was ∼6.5 m^2, and the length was ∼2.3 m. The granular filter was made by "head size" rocks. The volume average diameter was estimated to be ∼200 mm, and the void fraction was estimated to ∼0.47. A solid explosive charge was used to generate the shock wave. Two tests with two different charges were carried out (5 and 20 kg C-4). The charge was placed in the centre of the tunnel 10 m from the filter, which is about 4 tunnel diameters. This is somewhat close to the filter, but the availible tunnel length was limited. It was also necessary to have a certain

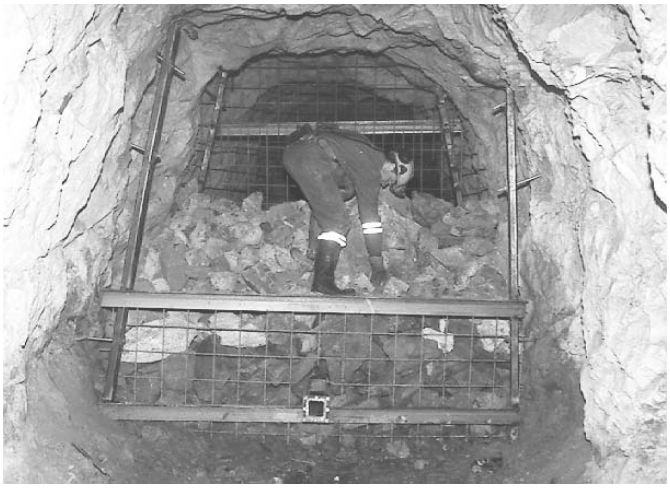

Fig. 4. Filter under construction

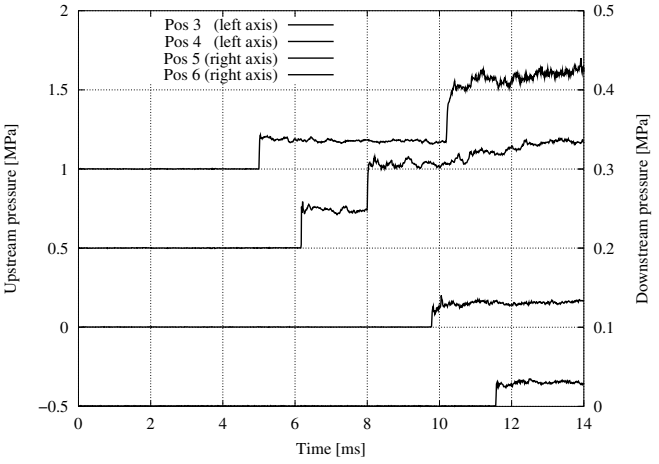

Fig. 5. Pressure record from Test 1. The pressure curves are shifted for better readability

free distance in the opposite direction to avoid reflection from that end to interfere with the primary shock wave.

A total of 12 pressure transducers were used for recording the pressures, six Kistler 603B, three Kulite HKS-11 and three Kulite XT-190. Six transducers were located upstream of the filter and six downstream. The Kistler and Kulite transducers were connected to two separate systems for data recording (three of each kind on each side of the filter). The data recording of the Kistler transducers was triggered by arrival of the shock wave at the first Kistler transducer, while the data recording of the Kulite transducers was triggered by a break-wire. Figure 3 shows a sketch of the experimental setup and the positions of the pressure transducers. The first number corresponds to the Kistler transducers and the second number to the Kulite transducers. Figure 4 shows a picture of the filter under construction. Further description of the experimental setup is given by Slungaard (2002).

3 Results

3.1 Shock tube

Determination of shock wave pressure from pressure records is subjected to an individual judgment of the person reading the record. A more objective method is to use the time of arrival of the shock front to calculate the velocity, and use the velocity to calculate the pressure.

Table 3 compares theoretical upstream shock pressure with measured pressure for the pressurized air driver tests. The pressures are mean values for experiments 1–12 shown in Table 5. As can be seen in Table 3, the deviation between theoretical and measured pressure is small. This indicates a nearly ideal rupture of the diaphragms, and that the shock wave has stabilized. Figure 5 shows an example of a pressure record from these tests (Test 1). Downstream of the filter a pressure rise behind the shock wave can be seen. This pressure rise is more pronounced with higher driver pressure and larger θ. A comparison between Test 1 and Test 12 in Fig. 6 shows this. In order to increase the

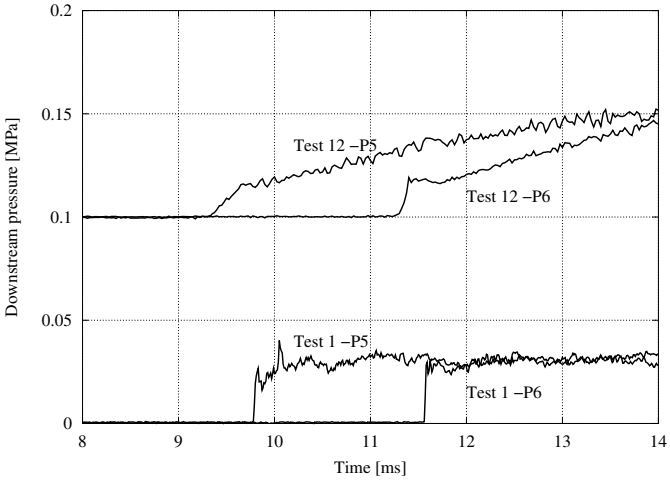

Fig. 6. Pressure record downstream of the filter for Test 1 and Test 12. The pressure curves are shifted for better readability

readability, only the two transducers closest to the filter on each side are shown. The right y-axis is used for the transducers downstream of the filter (P5 and P6).

Table 3. Comparison of theoretical and measured pressure

Driver pressure (MPa)	Theoretical pressure (MPa)	Pressure based on velocity[1)] (MPa)	Pressure from pressure record[2)] (MPa)
1	0.196	0.202	0.217
5	0.418	0.392	0.41

[1)] Mean velocity P1-P4.
[2)] Transducer P3

In the case of a pressurized air driver, the pressure upstream of the filter is calculated from the mean velocity between P1 and P4. When a solid explosive driver is used, the shock wave will be weakened much faster than when

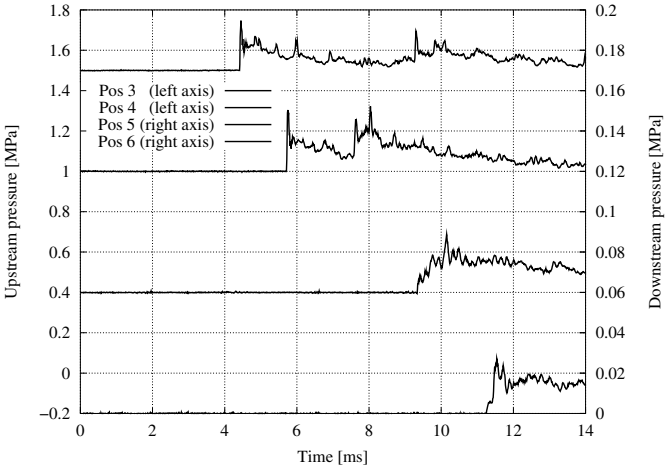

Fig. 7. Pressure record from Test 21. The pressure curves are shifted for better readability

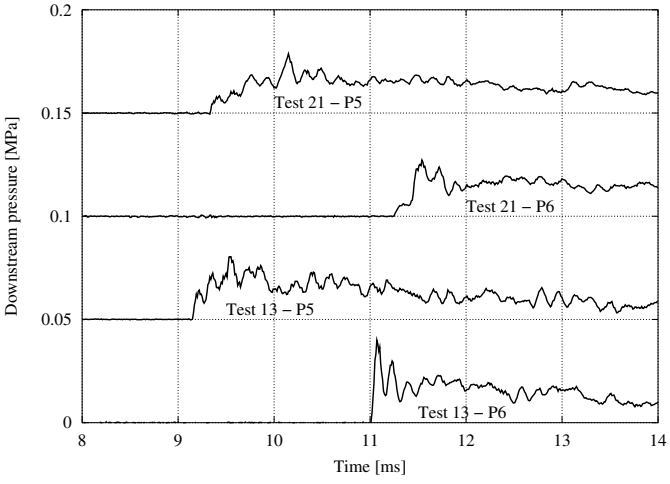

Fig. 8. Pressure record downstream of the filter for Test 13 and Test 21. The pressure curves are shifted for better readability

Table 4. Incoming pressure variation with solid explosives

C-4 (g)	Incoming pressure (min-max)[1)] (MPa)	Mean pressure[1)] (MPa)
10	0.143–0.173	0.158
30	0.267–0.350	0.304

[1)] Based on velocity between P3-P4.

using a pressurized air driver. The pressure upstream of the filter in these tests is therefore calculated from the velocity between P3 and P4. Downstream of the filter, the pressure is calculated from the velocity between P5 and P8 in both cases, since the shock strength is more or less constant here (i.e. the velocity of the shock wave is constant).

Although the weight of the explosive charges were carefully adjusted, there was some variation in incoming pressure for the same charge weight. This is shown in Table 4. The results for all these experiments (13–24) are shown in Table 5.

Table 5. Experimental results

Test	Driver	Filter length/ particle diameter (mm)	Incoming pressure[1)] (MPa)	Down-stream pressure[2)] (MPa)	Atten-uation P2/P1
Pressurized air					
1	1.0MPa	150/18.8	0.209	0.032	0.152
2	5.0MPa	150/18.8	0.389	0.074	0.189
3	1.0MPa	300/18.8	0.203	0.010	0.048
4	5.0MPa	300/18.8	0.403	0.017	0.042
5	1.0MPa	450/18.8	0.196	0.003[3)]	0.014
6	5.0MPa	450/18.8	0.378	0.050	0.013
7	1.0MPa	300/53.9	0.195	0.040	0.204
8	5.0MPa	300/53.9	0.387	0.084	0.215
9	1.0MPa	600/53.9	0.200	0.016	0.079
10	5.0MPa	600/53.9	0.404	0.034	0.083
11	1.0MPa	870/53.9	0.210	0.013	0.064
12	5.0MPa	870/53.9	0.389	0.012	0.030
Explosive charge					
13	10g	150/18.8	0.155	0.023	0.145
14	30g	150/18.8	0.350	0.031	0.088
15	10g	300/18.8	0.173	0.007	0.040
16	30g	300/18.8	0.282	0.008	0.029
17	10g	450/18.8	0.151	0.006	0.040
18	30g	450/18.8	0.267	0.014	0.052
19	10g	300/53.9	0.169	0.032	0.189
20	30g	300/53.9	0.305	0.055	0.179
21	10g	600/53.9	0.143	0.010	0.067
22	30g	600/53.9	0.314	0.016	0.051
23	10g	870/53.9	0.155	0.010	0.062
24	30g	870/53.9	0.305	0.005	0.016

[1)] Calculated from velocity measurements. P1-P4 for air driver and P3-P4 for solid driver

[2)] Calculated from velocity measurements (P5-P8)

[3)] Calculated from velocity measurements (P5-P6)

Figure 7 shows an example of the pressure records from these tests (Test 21). In contradiction to Fig. 5 there is no pressure rise after the passage of the reflected shock wave or behind the shock wave downstream of the filter. This is due to the change of driver type. Figure 8 shows a comparison of the pressure downstream of the filter for Test 13 and Test 21, with Test 21 having the largest θ.

3.2 Large scale

Only two tests were carried out at large scale. The results from these tests are shown in Table 6 and Fig. 10. The first test caused some minor damage to the filter, while the second test caused severe damage to the filter on the downstream side. The measurements are, however, assumed to be unaffected by the destruction of the filter, since this happens at a much longer timescale than the measurements.

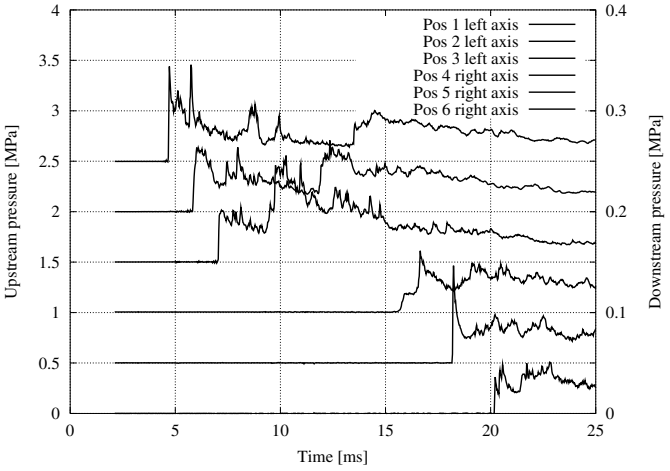

Fig. 9. Pressure record from the large scale test with 20 kg charge. The pressure curves are shifted for better readability

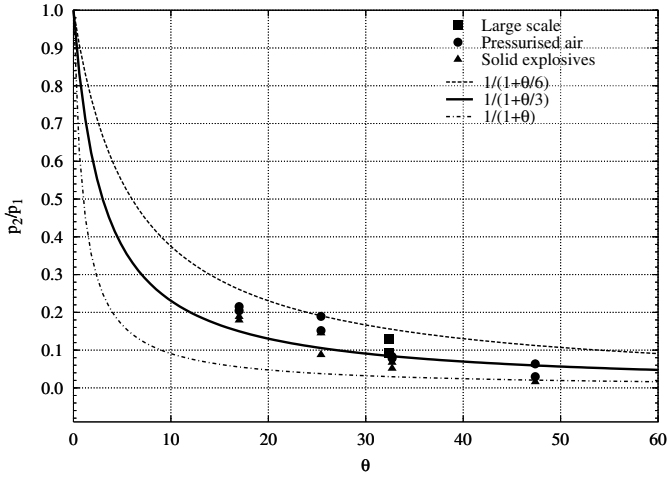

Fig. 10. Attenuation of shock waves as a function of the filter characteristic. Results from this study

Table 6. Experimental results large scale

Test	Charge C-4 (kg)	Incoming pressure[1)] (MPa)	Downstream pressure[1)] (MPa)	Attenuation P2/P1
1	5	0.175	0.017	0.097
2	20	0.450	0.063	0.140

[1)] Mean value of Kistler and Kulite transducers read from pressure plots

The pressures obtained with the two independent data recording systems, were in reasonable agreement, but with some variations. The mean velocity from the first transducer to the last transducer, however, agreed very well. The pressure record for Test 2 (Kulite transducers) are shown in Fig. 9.

4 Discussion and conclusion

With pressurized air driver, the impulse on the granular filter is much higher than with solid explosives. In some of these tests a small damage on the downstream side of the filter was observed.

In the large scale test with 20 kg C-4, the filter was seriously damaged on the downstream side due to a too weak filter support. On the upstream side, however, the filter support had no damage. This shows that special care should be taken in dimensioning the downstream filter support.

The reflection from the filter can easily be recognised in Fig. 9. There are also other pressure peaks prior to the reflection that can be seen. These pressure peaks are probably caused by reflections from the side walls. This clearly indicates that the shock is not stabilized. However, as Fig. 9 shows, these pressure peaks are reduced as the distance from the explosive charge increases.

In the shock tube experiments with pressurised air in the driver section, a pressure rise after the reflection of the shock wave from the upstream side of the filter can be seen. In this case, the length of the driver section is larger than the distance from the diaphragm to the granular filter which is about 10 tube diameters. This pressure rise is typical in a situation like this. With a shorter driver section and a longer distance from the diaphragm to the filter, this pressure rise would be diminished or even removed. This can be seen in the experiments by Slungaard (2002), where the distance between the diaphragm and the filter was about 35 tube diameters, while the driver section was about 10 tube diameters. The pressure behind the shock wave downstream of the filter also increases. This pressure rise is more pronounced with higher driver pressure and larger θ. A comparison between Test 1 and Test 12 in Fig. 6 shows this. The figure also shows that for Test 12 (largest θ) the shock wave gradually builds up from a pressure wave. This pressure rise behind the shock front can also be seen in the experiments by Slungaard (2002).

From Fig. 6 it is not obvious what pressure should be used when determining the shock wave attenuation. As previously described, in this study the shock velocities are used to calculate the pressure. However, when the pressure increases behind the shock front, the maximum pressure can be significantly higher than the pressure of the shock front.

All results from the present study are shown as a function of θ in Fig. 10. Figure 11 shows the experimental results compared with experimental results found in the literature. The results are plotted as p_2/p_1 against the characteristic of the granular filter (θ). For all tests f_m is assumed to be constant (1.0 for spheres or 2.5 for crushed rock). The results from the literature are read from plots with various x-axis parameters. These results are then recalculated and can, therefore, be somewhat uncertain. The interpretation of these pressure measurements are also unknown. All the experiments found in the literature are performed at a relatively small scale and with spherical particles. The results cover a broad range of θ (see Table 1).

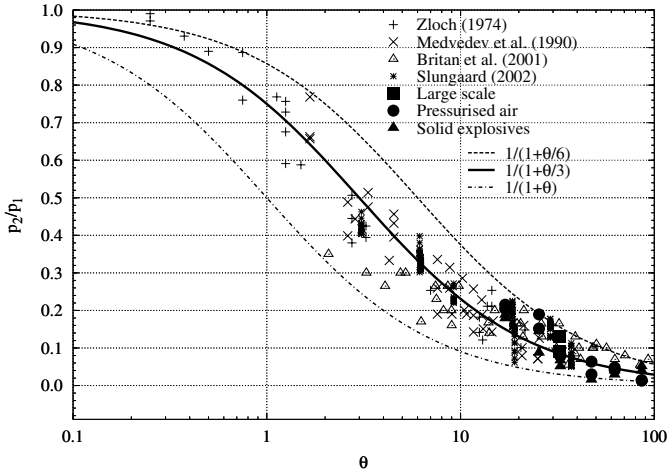

Fig. 11. Attenuation of shock waves as a function of the filter characteristic. Data are from this study and other studies

As pointed out by Britan et al. (2001) their data are below the data from Medvedev et al. (1990) for short filters ($\theta < 6$), and above for longer filters ($\theta > 20$). The data from Zloch (1976) are more in agreement with Medvedev et al. than with Britan et al. for the shortest filters tested by Britan et al. The data from this study are in agreement with the data from Britan et al. (2001) for the shortest filters in this study ($17 < \theta < 30$), but are below for the longest filters.

Small scale experiments previously performed by Slungaard (2002) with 15 and 42 mm glass balls are also shown. The experiments were performed in a square shock tube with internal dimensions 127×127 mm. The experiments ranges from $\theta = 3$ to 37.

As can be seen from Fig. 10 there is some scatter in the data. A possible reason for the scattering of the data are small gaps over the horizontal filters. A vertical shock tube would, therefore, be more ideal, but not as practical when the scale is large. However, also the data from Britan et al. (2001) and Medvedev et al. (1990), show the same scatter. In both these cases the shock tube was vertically oriented. Other reasons may be measurements or estimates of the void fraction and particle size, non-uniform void fraction, or interpretation of the pressure records.

By using the method of characteristics, Zloch (1976) found that attenuation of shock waves in tube bundles could be written as:

$$p_2/p_1 = 1/(1 + \theta/B) \tag{5}$$

where B is a function of the spesific heat ratio, the Mach number, the friction factor and the tube diameter. In this work, a correlation of the same form but with an experimentally adjusted and constant B-value is used. Figure 10 and 11 both show this equation as curves for different constant values of B.

The curves show that almost all results can be found between $1/(1+\theta/6) > p_2/p_1 > 1/(1+\theta)$. As can be seen, the scatter in the results are most pronounced for $\theta < 10$. The curve $1/(1+\theta/3)$ is very close to a best fit to all the results assuming an equation of this form.

The figure also shows that as θ increases, p_2/p_1 approaches zero. This can be achieved by an infinitely long filter or a filter with zero void fraction (i.e. a compact wall). In a practical situation selecting a filter with θ between 30 and 60 should give sufficient protection. Selecting a filter with θ larger than 60 will only give minor improvements to the filters capability to shock wave attenuation as shown in Fig. 10 and 11. Increasing the filter length, decreasing the particle diameter or reducing the void fraction will increase θ. This will, however, also increase the pressure drop with normal gas flow through the filter as shown by Eq. (3).

The following conclusions can be drawn:

- The results from these studies are in reasonable agreement with previous results and results found in the literature.
- The attenuation of the shock wave is approximately the same for both pressurised air and solid explosives driver.
- In all cases $p_2/p_1 = 1/(1 + \theta/6)$ will give a conservative estimate of the attenuation of a shock wave in a granular filter with filter characteristic θ found from Eq. (4).

Acknowledgements. The authors would like to thank The Norwegian Defence Estates Agency for both financial and practical support during the tests. The work done by the technical staff at the university is also higly appreciated. The staff at Norwegian Ammunition Disposal Company (NAD) did a great job when the large scale filter was built.

Appendix

Figure A.1 shows the results from Engebretsen et al. (1996) plotted in the same way as in Fig. 11. Most of these results lies above $p_2/p_1 = 1/(1 + \theta/6)$. However, all other experiments found in the literature, and this study, lies below this curve with a few exceptions lying just above.

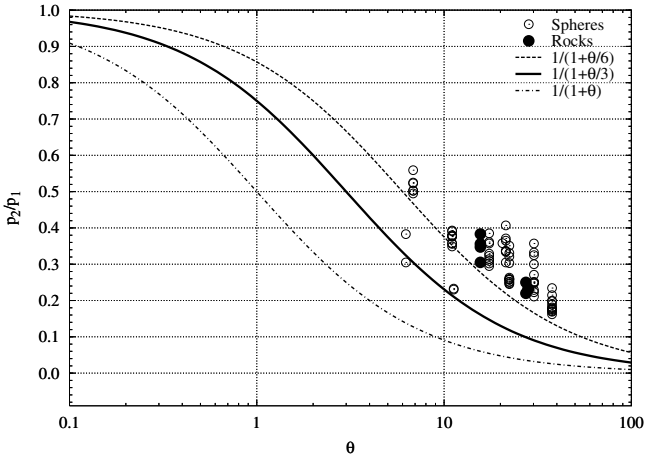

Fig. A.1. Attenuation of shock waves as a function of the filter characteristic. Data from Engebretsen et al. (1996)

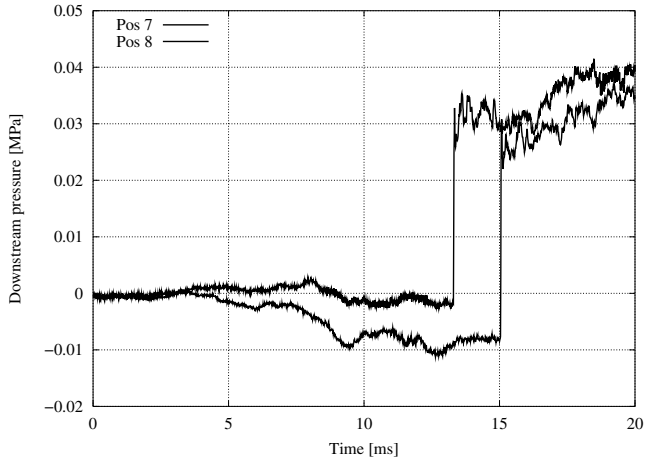

Fig. A.2. Pressure transducers drifting away from zero before arrival of the shock wave

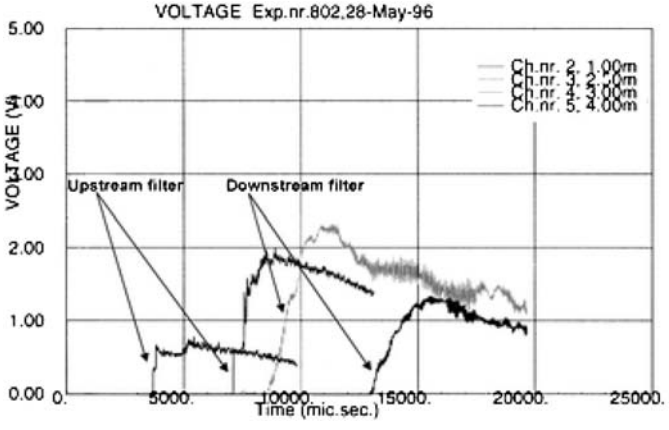

Fig. A.3. Example of voltage record of the data presented by Engebretsen et al. (1996). The distance between the transducers is 1.0 m

The experiments by Engebretsen et al. (1996) were recorded on a 10 MHz data logger with 8 bit vertical resolution. This data logger could not handle negative values. If the pressure signals drifted below zero before the arrival of the shock wave, this could not be registered. Figure A.2 shows an example of pressure transducers drifting away from zero. In order to give the correct pressure, the data have to be shifted up so that the shock wave starts at 0.0 MPa.

Engebretsen et al. used Kistler 412 transducers downstream of the filter. These transducers have a significantly lower frequency response compared to the 603B type, and no clear shock wave front could be seen downstream of the filter. As a consequence, maximum pressure downstream of the filter was used as the downstream pressure. Figure A.3 shows an example. This is in contrast to Slungaard (2002) who repeated the experiments with 15 mm spheres, but with Kistler 603B pressure transducers and a Yokogawa DL 708 digital oscilloscope. Clear downstream shock fronts could then be detected, and the shock wave velocity was used for calculating the shock strength. Slungaard (2002) also give a brief sensitivity analysis of different pressure interpretation methods.

When we look at the original data and try to calculate the velocity downstream of the filter, we find that in many cases the velocity is below M = 1. This is physically impossible for a pressure wave. The reason for this is that the time of arrival cannot be found when the signal is negative before arrival of the pressure wave. Figure A.3 shows this. In this example the velocity found from time of arrival at the two pressure transducers downstream of the filter is 227 m/s.

The pressure transducers and the data logger available at the time of the experiments are therefore responsible for these errors. Since drifting of the pressure signal below zero cannot be corrected, the downstream pressure levels recorded are also uncertain due to possible pressure signal drift that is not corrected for. As a consequence of this, *these experiments should not be referred in any future work.*

References

Bakken J (1995) Experimental and theoretical study of the effect of water on gaseous detonations and deflagrations – The Norwegian University of Science and Technology, Ph.D. thesis 1995:49

Britan A, Ben-Dor G, Igra O, Shapiro H (2001) Shock wave attenuation by granular filters. Journal of Multiphase Flow 27: 617–634

Engebretsen T, Bakken J, Hansen EWM, Lysberg I (1996) Shock waves and gas flow through granular materials – Proceedings from Explosion effects in granular materials, Oslo, Norway, August 1996, pp 111–131

Ergun S (1952) Fluid flow through packed columns, Chem Eng Progress 48

Idelchik IE (1994) Handbook of hydraulic resistance, 3rd edn. CRC Press, Boca Raton, Ann Arbor, London, Tokyo, pp 503–539

Macdonald IF, El-Sayed MS, Mow K, Dullien FAL (1979) Flow through porous media – the Ergun equation revisited - Ind Eng Chem Fundam 18, 199–208

Medvedev SP, Frolov SM, Gelfand BE (1990) Attenuation of shock waves by screens of granular material. Journal of Engineering Physics (English translation of Inzhenerno-Fizicheskii Zhurnal) 59, 714–718

Slungaard T, Bakken, J, Engebretsen, T (1998) Measurements and prediction of the hydraulic resistance of granular materials. Proceedings from Transient loading and response of structures, Trondheim, Norway, July 1998, pp 671–683

Slungaard T (2002) Hydraulic resistance, shock wave attenuation and gaseous detonation extinction in granular materials. The Norwegian University of Science and Technology, Ph.D. thesis 2002:65

Zloch N (1976) Shock attenuation in beds of granular solids. Archives of Mechanics 28: 817–825